A data-driven approach to predict the attachment density of biofouling organisms

Andre E. Vellwock[a], Jimin Fu[a], Yuan Meng[b], V. Thiyagarajan[b], Haimin Yao[a,*]

[a]*Department of Mechanical Engineering, The Hong Kong Polytechnic University, Hung Hom, Kowloon, Hong Kong SAR, China*

[b]*The Swire Institute of Marine Sciences and School of Biological Sciences, The University of Hong Kong, Hong Kong SAR, China*

[*]Corresponding author, E-mail address: mmhyao@polyu.edu.hk (H. Yao)

A data-driven approach to predict the attachment density of biofouling organisms

Abstract

The attachment efficiency of biofouling organisms on a solid surface depends on a variety of factors including species of the fouler, nutrition abundance, salinity, temperature, flow rate, surface morphology and mechanical properties of the solid to be attached and so on. So far, extensive research has been carried out to investigate the effects of these factors on the attachment behavior for various fouling species. However, the obtained results are normally species-dependent and seemly scattering. There is no universal rule that can be applied to predict the attachment efficiency under given conditions. To solve this problem, in this paper we carry out a meta-analysis on the effects of 10 selected factors on the attachment efficiency, resulting in a universal quantitative correlation between the attachment density and the selected factors. This obtained correlation is experimentally validated by an attachment test of tubeworms (*Hydroides elegans*) on PDMS surfaces with controllable stiffness. Our results provide a practical approach to quantitatively predict the attachment efficiency of fouling organisms and should be of great value to the design of anti-biofouling materials and structures.

Keywords: marine biofouling, meta-analysis, dimensional analysis, regression, anti-biofouling, surface topography

Introduction

Marine biofouling refers to the undesirable attachment and accumulation of marine organisms on solid structures submerged in the ocean. The attachment of biofouling organisms on solid surfaces is a complex biochemical process affected not only by environmental variables such as temperature, salinity, pH value, flow rate, nutrition abundance but also by the structural and physical features of the solid to be attached such as its surface morphology and stiffness. Understanding the dependence of biofouling attachment on these influencing factors will be of great value to the effective control of biofouling. So far, extensive studies have been carried out to investigate the attachment behavior of diverse biofouling species under different controlled conditions. Qian et al. (2000) found that water flow rate directly affects the attachment of biofoulers. Moreover, such influence exhibits species dependence. For example, at flow rates higher than 50 cm s^{-1} the cryptic *Bugula neritina* is still able to attach to the studied surface, while *Hydroides elegans* cannot. High flow rate not only reduces the engaging time of a larva for settlement on a surface but also increases the resultant drag force and affect the growth of biofilms. Thorson (1964) studied the effect of irradiance level on the attachment density on 141 fouler species and showed that 94% are phototactic. Nevertheless, it was shown that fouling organisms tend to avoid direct contact with sunlight, resulting in a non-linear distribution through the seawater depth. Howes et al. (2007) confirmed that the larvae attachment density of the ascidian *Ciona intestinalis* is higher at depths between 4.5m to 8.5m. Further, Lehaitre (2008) indicated that the upsurge of foulers around decks and anchored boats can be attributed to the sufficient provision of nutrients around coastal areas as a result of organic matter decomposition (micro-organisms or detritus). In laboratory experiments conditions, nutrition abundance relies on the amount of feeding, the population of foulers, and the volume of the water tank.

In addition to the environmental factors, the attachment density of organisms is influenced by the larvae and surface attributes. Scardino et al. (2008) studied multiples species attachment response to surfaces microfeatures and concluded that the characteristic size of larvae is essential to their attachment location choice. Similar results were found by Callow et al. (2002) and Schumacher, Carman, et al. (2007). Recently, Fu et al. (2018) developed a theory which explained the attachment of foulers through contact mechanics, validating the significance of larvae and surface's features dimensions. The latter also implied that not only the surface morphology but also its elastic properties are important. Indeed, Ahmed et al. (2011) analyzed the settlement of the barnacle *Balanus amphitrite* on PDMS surfaces with different elastic properties and found lower attachment densities on surfaces with reduced elastic moduli. Moreover, Gabilondo et al. (2013) studied tubeworm *Ficus enigmaticus* and showed a quasi-linear increase of the attachment density of larvae with the testing time ranging from 24 h to 96 h.

Despite these findings and achievements, it is still extremely challenging to draw a general conclusion of how different influencing factors affect the attachment efficiency of fouling organisms, because the results obtained are species-dependent and scattering.

It is still unclear if there is a universal rule governing the attachment efficiency of biofouling organisms. In view of these problems, here we propose a data-driven method in an attempt to correlate the attachment density, a quantity characterizing the efficiency of attachment, and multiple influencing factors. Meta-analysis is carried out based on the published results of multiple studies on different species irrespective of their specific attachment mechanisms (Qian et al. 2000; Callow et al. 2002; Scardino et al. 2006; Schumacher, Aldred, et al. 2007; Schumacher, Carman, et al. 2007; Scardino et al. 2008; Ahmed et al. 2011; Gabilondo et al. 2013; Brzozowska et al. 2014; Vucko et al. 2014; Mincheva et al. 2016; Fu et al. 2018). It is our goal to find a general quantitative description of the attachment density as a function of multiple influencing factors.

Buckingham π theorem

In engineering, applied mathematics, physics, and biology, Buckingham π theorem (Buckingham 1914) is a widely-applied theorem for dimensional analysis. The theorem states that if there is a physically meaningful equation involving a certain number n of physical variables, then the original equation can be rewritten in terms of a set of $p = n - m$ dimensionless variables (or parameters) Π_i (i =1, ⋯, p), which are referred to as "Π groups" and can be constructed from the original variables (Buckingham 1914). Here, m is the number of physical dimensions of the problem involved (*e.g.*, length, mass, time). The selection of the dimensionless parameters Π_i (i =1,⋯, p) is not unique. Buckingham π theorem provides a method to construct these dimensionless parameters from the given variables, even though the form of the original equation remains unknown. This feature makes the theorem quite applicable to the biofouling problem whose determinants and the physics involved has not been fully understood yet.

To identify the parameters affecting the attachment of fouling organisms, let us make a review of the settlement test that is commonly adopted to characterize the attachment efficiency of a biofouling species. **Figure 1** shows a typical experimental setup for the settlement test, in which a testing plate is mounted on the bottom of a tank full of filtered seawater simulating the marine environment. A given number of larvae of a specific fouling species are placed into the tank and nurtured with necessary food feeding and lighting. Sometimes, circulating seawater is introduced into the tank to simulate the effect of flow rate in the real marine environment. After a given period of time, the testing plate is taken out from the tank and the number of attached fouling organisms is counted. The attachment density (a), which is defined as the number of attached organisms per unit area, is used to characterize the attachment efficiency. Reducing attachment density is the common objective of most anti-biofouling endeavors. In this simplified experimental model, the conceivable parameters that affect the attachment density include the concentration of available larvae (ρ), experiment time (t), flow rate (Q), irradiance level of lighting (W), nutrition abundance in the seawater which is related to the tank volume (V). Recent studies indicated that the elastic modulus (E) and surface morphology of the material being attached also play an important role in determining the attachment efficiency (Ahmed et al. 2011; Fu et al. 2018). For a solid surface with regular morphology, wavelength (λ) and asperity depth (h) are two important characteristic length scales that should be considered especially in a relative sense to the characteristic size of the organism (D). Additionally, there are other parameters that may also affect the attachment efficiency such as pH value, salinity and temperature. However, these factors are not considered in this study because they varied little in the biofouling tests done under laboratory conditions.

Above description of the determining factors in a typical biofouling test in laboratory allows us to proceed further with the Buckingham theorem. In our case, we have 10 variables and 3 dimensions, and according to the theorem, 7 dimensionless groups are established as follows:

$$\Pi_1 = a \cdot D^2, \Pi_2 = \frac{E \cdot D}{W \cdot t}, \Pi_3 = \frac{h}{D}, \Pi_4 = \rho \cdot D^3, \Pi_5 = \frac{\lambda}{D}, \Pi_6 = \frac{Q \cdot t}{D^2}, \Pi_7 = \frac{V}{D^3}$$

The values of many Π groups above are distributed in a wide range from zero to 10^6 (see **Table 1**), hence taking the natural logarithm of all terms is appropriate. Additionally, to avoid the possible mathematical undefinition, a constant of unity is added to the terms that may take zero. Therefore, a new set of dimensionless groups are defined as follows:

$$\widetilde{\Pi}_1 = \ln(a \cdot D^2), \widetilde{\Pi}_2 = \ln\left(\frac{E \cdot D}{(1+W) \cdot t}\right), \widetilde{\Pi}_3 = \ln\left(\frac{1+h}{D}\right), \widetilde{\Pi}_4 = \ln(\rho \cdot D^3)$$

$$\widetilde{\Pi}_5 = \ln\left(\frac{1+\lambda}{D}\right), \widetilde{\Pi}_6 = \ln\left(\frac{(1+Q) \cdot t}{D^2}\right), \widetilde{\Pi}_7 = \ln\left(\frac{V}{D^3}\right)$$

In these groups, $\widetilde{\Pi}_1$, which is correlated to the attachment density, is regarded as a function of the other six groups or variables, namely,

$$\tilde{\Pi}_1 = f(\tilde{\Pi}_2, \tilde{\Pi}_3, \tilde{\Pi}_4, \tilde{\Pi}_5, \tilde{\Pi}_6, \tilde{\Pi}_7) \qquad (1)$$

In the following, the form of function *f* will be determined by regression analysis based on the 215 datasets from 12 published papers as summarized in **Appendix A**.

Regression analysis

Regression analysis is a technique used to seek the relationship between one or more independent variables and a dependent variable. In our case, we assume that the effect of each independent variable is additive. The predicted value of the dependent variable, $\hat{\tilde{\Pi}}_1$, thus can be approximated as a quadratic polynomial function of the independent variables $\tilde{\Pi}_i$ (i=2, …, 7)

$$\hat{\tilde{\Pi}}_1 = k_1 + \sum_{i=2}^{7} k_{\mathrm{i}} \cdot \tilde{\Pi}_{\mathrm{i}} + \sum_{i=2}^{7} \sum_{j=i}^{7} k_{\mathrm{ij}} \cdot \tilde{\Pi}_{\mathrm{i}} \cdot \tilde{\Pi}_{\mathrm{j}} \qquad (2)$$

where coefficients k_{i} (i = 1, ⋯,7) and k_{ij} (i, j = 2, ⋯,7) are to be determined via regression. Eq. (2) can be deemed as the second-order approximation of the function *f* in Eq. (1). The widely applied method to determine the coefficients in an assumed expression is ordinary least square (OLS), which tends to be sensitive to the data peculiarities such as outliers, multicollinearity and heteroscedasticity. For examples, in the OLS method all inputs are equally weighted and thus uniformly important. In our case, outliers are naturally present. Moreover, due to the inclusion of some variables, such as diameter *D*, in multiple *Π* groups, multicollinearity also exists. The existence of outliers and multicollinearity would generate abnormal data distribution. Under such circumstance, robust regression methods should be applied as they require less restrictive assumptions to calculate the regression coefficients (Bagheri and Midi 2009; Lambert-Lacroix and Zwald 2011).

Consider a summation of $\sum_{m=1}^{N} \delta\left(\frac{e_m}{s}\right)$, where e_m stands for the residual given by

$$e_m = \tilde{\Pi}_{1,m} - \hat{\tilde{\Pi}}_{1,m} = \tilde{\Pi}_{1,m} - \left(k_1 + \sum_{\mathrm{i=2}}^{7} k_i \cdot \tilde{\Pi}_{i,m} + \sum_{\mathrm{i=2,j=2}}^{7,7} k_{ij} \cdot \tilde{\Pi}_{i,m} \cdot \tilde{\Pi}_{j,m}\right)$$

and $s = \frac{\mathrm{median}|e_m - \mathrm{median}|e_m||}{0.6745}$. Here, function $\delta(\cdot)$ stands for the likelihood function of the distribution of the residuals. Following Huber's method (Huber 1964), we take

$$\delta(z) = \begin{cases} z^2, & |z| < c \\ |2z|c - c^2, & |z| \geq c \end{cases} \text{ with } c = 1.345$$

By minimizing the summation $\sum_{m=1}^{N} \delta\left(\frac{e_m}{s}\right)$, the coefficients k_i (i = 1, ⋯,7) and k_{ij} (i = 2, ⋯,7; j = i, ⋯,7) can be determined by solving the following derivative equations

$$\frac{\partial\left[\sum_{m=1}^{N} \delta\left(\frac{e_m}{s}\right)\right]}{\partial k_\mathrm{i}} = 0, (i = 1, \cdots, 7)$$

$$\frac{\partial\left[\sum_{m=1}^{N} \delta\left(\frac{e_m}{s}\right)\right]}{\partial k_{ij}} = 0, (i = 2, \cdots, 7; j = i, \cdots, 7)$$

Above algorithm has been incorporated into the NCSS (2019) statistical software, by which we carried out the regression based on the published data in the literature mentioned above.

Results and discussions

The values of all coefficients obtained from the above-mentioned robust regression are shown in **Table 2** together with their corresponding p-values which indicate whether the correlation between the dependent variable $\widetilde{\Pi}_1$ and the corresponding independent variable is significant or not. Normally, 0.05 is adopted as the threshold for significance. If *p*-value is less than 0.05, the correlation between them is deemed significant. For example, the p-values corresponding to k_2, k_4, k_7, k_{22}, k_{44}, and k_{77} are close to zero, implying that the substrate stiffness, larvae concentration (ρ) and the container volume (V) significantly determine the attachment density (a).

Figure 2a shows the values of $\widetilde{\Pi}_1$ predicted by the regression expression in comparison with the experimental observations. It can be seen that most of the data points are distributed around the line of $y = x$ irrespective of the fouling species, implying the strong and universal prediction competence of the regression expression of Eq. (2). To further investigate the quality of the regression results, **Figure 2b** shows the distribution of the residuals between the predicted data and their experimental counterparts. The highest frequency peak in the vicinity of zero indicates that most of the residuals are zero and the regression expression agrees well with the experimental results. The curve shows a Gaussian-like distribution. As stated before, our data possess outliers, which are evident here. By using a robust regression, we reduced the count of non-zero residuals and therefore reduced their impact. The distribution of the residuals in the spaces of each independent variable, $\widetilde{\Pi}_i (i = 2, \cdots, 7)$, and their products, $\widetilde{\Pi}_i \cdot \widetilde{\Pi}_j (i, j = 2, \cdots, 7)$, are plotted in Figure S1.

To further evaluate the quality of regression, we calculated the coefficient of determination (R^2), and the predicted residual error sum of squares (PRESS) R^2 (see Error! Reference source not found.). Both R^2 and PRESS R^2 are close to 1.0, implying the high quality of our regression.

After predicting $\widetilde{\Pi}_1$, the attachment density can be easily calculated through

$$a = \exp(\widetilde{\Pi}_1)/D^2$$

The regression results obtained above allows us to predict the dependence of attachment density on different determining factors quantitively for different species with distinct characteristic sizes and contrasting attachment mechanisms. For instance, take the characteristic sizes of four foulers: barnacle *B. neritina*, tubeworm *H. elegans*, algae *C. clavulatum* and *U. linza* as 321 µm, 200 µm, 37 µm and 5 µm, respectively. **Figure 3a** shows the dependence of attachment density on the stiffness of the substrate (E). Here, we assume that the substrate is flat with $h = \lambda = 0$ under laboratory light irradiance (W = 7.95 W/m^2), steady seawater conditions ($Q = 0$) in a container of 10 ml with an initial larvae concentration of 5 per ml. The total time for attachment was set as t = 48 h. Results in **Figure 3a** indicate the consentaneous effect of low substrate stiffness in reducing the attachment density of all organisms. Therefore, in marine industry, applying soft paint on ship hulls is expected to reduce the attachment of fouling organisms. **Figure 3b** shows the effect of flow rate on the attachment density of different species on a given substrate with stiffness E = 2 MPa and surface topography characterized by $h = \lambda$ = 10 µm. It is assumed that 1000 fouling organisms are added in a container of 100 ml. It is clear to see that flow rates higher than 4 cm/s will drastically reduce the attachment density and essentially eradicate it when above 8 cm/s, irrespective for all fouling species, implying that marine ships tend to be fouled when they are anchored or voyaging at low speed.

Figure 3c displays the effect of surface asperity height (h) of the substrate on the attachment density. Here, we assume that V = 10 ml, ρ = 10 ml^{-1} and surface wavelength λ = 10 µm. It can be seen that the attachment density of barnacles *B. neritina* (D = 321 µm) is insensitive to the asperity height at all. However, for tubeworms *H. elegans* (D =

200 μm), the attachment density increases as the asperity height increases and saturates when h = 21 μm. In contrast, the attachment density of algae *C. clavulatum* (D = 37 μm) exhibits the maximum value when the asperity height is approximately 50 μm, while the attachment density of *U. linza* (D = 5 μm) drops drastically with the increase of asperity height. In addition, **Figure 3d** presents the impact of surface wavelength while setting asperity height h = 10 μm. Except for tubeworms *H. elegans* (D = 200 μm) that has a peak of attachment density when wavelength λ = 8 μm, the prevailing behavior is to reduce attachment density when increasing surface wavelength.

To verify the capability of the above model in predicting the attachment density of fouling species, an attachment test was carried out by using tubeworms (see Methods for the details). **Figure 4** shows the experimental measurement of the attached density of the tubeworms on PDMS substrates with different stiffnesses in comparison to the prediction given by the above regression model. The small difference between them implies the applicability of our model in predicting the effect of substrate stiffness on the attachment efficiency of tubeworms.

Conclusions

In this paper, we successfully developed an empirical method to reveal the quantitative dependence of attachment density of biofouling species on a series of determining factors. Buckingham π theorem and robust regression were applied to determine the regression expression from the existing published datasets in literature. The obtained empirical expression from such meta-analysis shows a versatile competence in predicting the attachment density of biofoulers irrespective of the fouling species, laboratory conditions and substrate stiffness. Our model not only provides an approach to predict the attachment efficiency of a variety of fouling species on different kinds of substrates but also indicates the directions of antifouling efforts in naval industry.

Methods

Tubeworms attachment test

Tubeworms (*Hydroides elegans*) were collected from a fisherman's farm from Kei Ling Ha Lo Wai in Hong Kong (22°25'27.5"N, 114°16'39.5"E). The calcareous tubes were manually broken, and each worm was placed into 100 µl filtered seawater (0.22 µm mesh size) for eggs or sperms release. To promote fecundation, eggs and sperms were transferred to a single container with filtered seawater. Fertilized eggs were kept at 20°C in a 12L:12D cycle of lighting and daily fed with *Isocrysis albana*. After 6 days, the tubeworm larvae were ready for the attachment test. Testing PDMS specimens were placed in Petri dishes containing 10 ml seawater and 50 tubeworm larvae. Artificial stimuli were applied (CsCl, 5mmol/l) to induce settlement. Irradiance was calculated as 7.96 W/m^2. After 48h, the specimens were rinsed by seawater and the attached tubeworms were counted with the aid of an optical microscope.

Fabrication of PDMS specimens and nanoindentation tests

Four PDMS/hardener ratios were adopted: 1:20, 1:15, 1:10 and 1:5 to fabricate PDMS specimens of different stiffnesses. Nanoindentation tests (Hysitron TI900) were performed to measure the modulus of the fabricated PDMS specimens. Berkovich tip and a maximum load of 30 μN were applied. The results are displayed in **Table 4** .

Data availability statement

The data that support the findings of this study are openly available in Mendeley Data at http://dx.doi.org/10.17632/f5rbkd4482.2, DOI: 10.17632/f5rbkd4482.2.

Acknowledgments

The work was supported by the General Research Fund from Hong Kong RGC (PolyU 152193/14E). A.V. thanks Shu Gao for her help in figure production.

Declaration of interest statement

The authors declare no conflict of interest.

References

Ahmed N, Murosaki T, Kakugo A, Kurokawa T, Gong JP, Nogata Y. 2011. Long-term in situ observation of barnacle growth on soft substrates with different elasticity and wettability. Soft Matter. 7(16):7281.

Bagheri A, Midi H. 2009. Robust Estimations as a Remedy for Multicollinearity Caused by Multiple High Leverage Points. Journal of Mathematics and Statistics. 5(4):311-321.

Baur E, Osswald TA, Rudolph N. 2019. Material Properties. In: Baur E, Osswald TA, Rudolph N. Plastics Handbook. Hanser; p. 625-663.

Brzozowska AM, Parra-Velandia FJ, Quintana R, Xiaoying Z, Lee SSC, Chin-Sing L, Jańczewski D, Teo SLM, Vancso JG. 2014. Biomimicking Micropatterned Surfaces and Their Effect on Marine Biofouling. Langmuir. 30(30):9165-9175.

Buckingham E. 1914. On Physically Similar Systems; Illustrations of the Use of Dimensional Equations. Phys Rev. 4(4):345-376.

Callister WD. 2005. Fundamentals of materials science and engineering : an integrated approach. 2nd ed. Hoboken, N.J.: Wiley.

Callow ME, Jennings AR, Brennan AB, Seegert CE, Gibson A, Wilson L, Feinberg A, Baney R, Callow JA. 2002. Microtopographic Cues for Settlement of Zoospores of the Green Fouling Alga Enteromorpha. Biofouling. 18(3):229-236.

Davidson M, Steve Bastian, and Finley Markley. 1992. Measurement of the Elastic Modulus of Kapton Perpendicular to the Plane of the Film at Room and Cryogenic Temperatures. Supercollider 4.1039-1045.

Fu J, Zhang H, Guo Z, Feng D, Thiyagarajan V, Yao H. 2018. Combat biofouling with microscopic ridge-like surface morphology: a bioinspired study. Journal of The Royal Society Interface. 15(140):20170823.

Gabilondo R, Graham H, Caldwell GS, Clare AS. 2013. Laboratory culture and evaluation of the tubeworm Ficopomatus enigmaticus for biofouling studies. Biofouling. 29(7):869-878.

Howes S, Herbinger CM, Darnell P, Vercaemer B. 2007. Spatial and temporal patterns of recruitment of the tunicate Ciona intestinalis on a mussel farm in Nova Scotia, Canada. J Exp Mar Biol Ecol. 342(1):85-92.

Huber PJ. 1964. Robust Estimation of a Location Parameter. Ann Math Statist. 35(1):73-101.

Lambert-Lacroix S, Zwald L. 2011. Robust regression through the Huber's criterion and adaptive lasso penalty. Electronic Journal of Statistics. 5(0):1015-1053.

Lehaitre M, Delauney, L., Compere, C. 2008. Biofouling and underwater measurements. Paris, France: United Nations Educational, Scientific and Cultural Organization.

McKeen LW. 2014. Chapter 8, Thermoplastic Elastomers. In: McKeen LW. The Effect of Temperature and other Factors on Plastics and Elastomers. 3rd ed. Oxford, UK: William Andrew Publishing; p. 371-398.

Mincheva R, Beigbeder A, Pettitt ME, Callow ME, Callow JA, Dubois P. 2016. Metal-free anti-biofouling coatings: the preparation of silicone-based nanostructured coatings via purely organic catalysis. Nanocomposites. 2(2):51-57.

NCSS L. 2019. NCSS 2019 Statistical Software. Kaysville, Utah, USA.

Qian P, Rittschof D, Sreedhar B. 2000. Macrofouling in unidirectional flow: miniature pipes as experimental models for studying the interaction of flow and surface characteristics on the attachment of barnacle, bryozoan and polychaete larvae. Marine Ecology Progress Series. 207:109-121.

Scardino AJ, Guenther J, Nys Rd. 2008. Attachment point theory revisited: the fouling response to a microtextured matrix. Biofouling. 24(1):45-53.

Scardino AJ, Harvey E, Nys RD. 2006. Testing attachment point theory: diatom attachment on microtextured polyimide biomimics. Biofouling. 22(1):55-60.

Schumacher JF, Aldred N, Callow ME, Finlay JA, Callow JA, Clare AS, Brennan AB. 2007. Species-specific engineered antifouling topographies: correlations between the settlement of algal zoospores and barnacle cyprids. Biofouling. 23(5):307-317.

Schumacher JF, Carman ML, Estes TG, Feinberg AW, Wilson LH, Callow ME, Callow JA, Finlay JA, Brennan AB. 2007. Engineered antifouling microtopographies – effect of feature size, geometry, and roughness on settlement of zoospores of the green alga Ulva. Biofouling. 23(1):55-62.

Thorson G. 1964. Light as an ecological factor in the dispersal and settlement of larvae of marine bottom invertebrates. Ophelia. 1(1):167-208.

Vellwock AE. 2019. Biofouling studies dataset. 2 ed. Mendeley Data.

Vucko MJ, Poole AJ, Carl C, Sexton BA, Glenn FL, Whalan S, de Nys R. 2014. Using textured PDMS to prevent settlement and enhance release of marine fouling organisms. Biofouling. 30(1):1-16.

Wang Z, Volinsky AA, Gallant ND. 2015. Nanoindentation study of polydimethylsiloxane elastic modulus using Berkovich and flat punch tips. Journal of Applied Polymer Science. 132(5):41384.

Wypych G. 2015. PVC Properties. In: Wypych G. PVC Formulary. 2nd ed. San Diego: ChemTec Publishing; p. 5-44.

Appendix A

Database and assumptions

The datasets applied in this paper are from 12 published papers (Qian et al. 2000; Callow et al. 2002; Scardino et al. 2006; Schumacher, Aldred, et al. 2007; Schumacher, Carman, et al. 2007; Scardino et al. 2008; Ahmed et al. 2011; Gabilondo et al. 2013; Brzozowska et al. 2014; Vucko et al. 2014; Mincheva et al. 2016; Fu et al. 2018) and it is available online (Vellwock 2019). However, the values of some influencing variables may have not been explicitly indicated in some studies. Under such circumstance, inference should be carried out to estimate the value of that variable. In our study, the following inferences have been made:

(1) In Fu et al. (2018) the irradiance was not indicated. However, as it was a research carried out in our lab, we estimated the irradiance on the surface by inquiring the lamp potency and its distance to the experiment. As a representative laboratory condition, such value of irradiance was also adopted for the studies of Ahmed et al. (2011); Gabilondo et al. (2013); Brzozowska et al. (2014); Vucko et al. (2014).

(2) In Qian et al. (2000), the volume of tank was estimated as 4000 ml, equal to the "head tank" described in the paper.

(3) The features' geometries in the studies by Schumacher, Aldred, et al. (2007); Schumacher, Carman, et al. (2007) have distinct features along different axes. Howbeit, we took the lateral period as λ.

Moreover, the stiffness of substrate in each attachment test was estimated, as shown in **Table A1** below.

Table A 1. Estimation of the material stiffness

Material	**Elastic modulus [MPa]**	**Reference**	**Applied to data from**
PDMS	2	Wang et al. (2015)	Callow et al. (2002); Schumacher, Aldred, et al. (2007); Schumacher, Carman, et al. (2007); Gabilondo et al. (2013); Vucko et al. (2014); Fu et al. (2018)

Glass	70000	Callister (2005)	Qian et al. (2000); Gabilondo et al. (2013); Brzozowska et al. (2014); Fu et al. (2018)
Polyimide	2700	Davidson (1992)	Scardino et al. (2006); Scardino et al. (2008)
Polycarbonate	2100	Baur et al. (2019)	Scardino et al. (2006); Scardino et al. (2008)
Polystyrene	3000	Callister (2005)	Ahmed et al. (2011); Gabilondo et al. (2013)
Polyvinyl chloride*	8	Wypych (2015)	Qian et al. (2000)
Polyethylene	200	Baur et al. (2019)	Qian et al. (2000)
Polyurethane	7	McKeen (2014)	Qian et al. (2000)
Polytetrafluoroethylene	500	Callister (2005)	Qian et al. (2000)

*All the PVCs stated in the paper were assumed to have the same elastic modulus.

Table 1. Practical ranges of the independent variables

Quantities	**Unit**	**Lower limit**	**Upper limit**
Available larvae concentration (*ρ*)	1/ml	0.02	3×10^6
Organism size (*D*)	µm	2	321
Surface wavelength (*λ*)	µm	0	800
Asperity height (*h*)	µm	0	650
Surface elastic modulus (*E*)	MPa	1	70000
Seawater flow rate (*Q*)	cm/s	0	31.9
Seawater volume (*V*)	ml	0.1	4000
Time (*t*)	hour	1	168
Light irradiance (*W*)	W/m^2	0	17.4

Table 2. Results of robust regression

Coefficient	Regression value	p-value	Coefficient	Regression value	p-value
k_1	-2.01913	0.1077	k_{34}	-0.08266	0.0292
k_2	0.69742	0.0077	k_{35}	0.14724	0.0761
k_3	-0.18372	0.6190	k_{36}	0.00625	0.9658
k_4	4.17394	0.0000	k_{37}	-0.16189	0.0202
k_5	-0.10871	0.7273	k_{44}	-0.20887	0.0000
k_6	0.04582	0.9220	k_{45}	-0.01309	0.6593
k_7	3.91912	0.0000	k_{46}	-0.40882	0.0000
k_{22}	-0.0329	0.0019	k_{47}	-0.11437	0.0001
k_{23}	-0.03353	0.6946	k_{55}	-0.06935	0.1380
k_{24}	-0.0505	0.0141	k_{56}	-0.08815	0.3789
k_{25}	0.02279	0.7418	k_{57}	0.01828	0.7248
k_{26}	-0.0986	0.0113	k_{66}	-0.33666	0.0000
k_{27}	-0.0022	0.8964	k_{67}	-0.07759	0.1190
k_{33}	-0.08884	0.1378	k_{77}	0.04203	0.0090

Table 3. Quality of regression

Quantities	Definition	Value
Coefficient of determination (R^2)	$1-\frac{\sum_{m=1}^{N}(f_m-\bar{\bar{\tilde{\Pi}}}_{1,m})^2}{\sum_{m=1}^{N}(\tilde{\Pi}_{1,m}-\bar{\bar{\tilde{\Pi}}}_{1})^2}$	0.9809
PRESS (Predicted residual error sum of squares) R^2	$1-\frac{\sum_{m=1}^{N}(\tilde{\Pi}_{1,m}-f_{m(m)})^2}{\sum_{m=1}^{N}(\tilde{\Pi}_{1,m}-\bar{\bar{\tilde{\Pi}}}_{1})^2}$	0.9486

Here, f_m stands for the m^{th} response value given by the function f which is obtained by regression on the basis of all N datasets; $f_{m(m)}$ stands for the m^{th} response value given by the function f which is obtained by regression on the basis of datasets with the m^{th} one excluded individually.

Table 4. Variations on the surfaces' modulus due to different PDMS/hardener ratios

PDMS/Hardener ratio	**Modulus [MPa]**
1:20	4.335
1:15	1.867
1:10	1.712
1:5	1.132

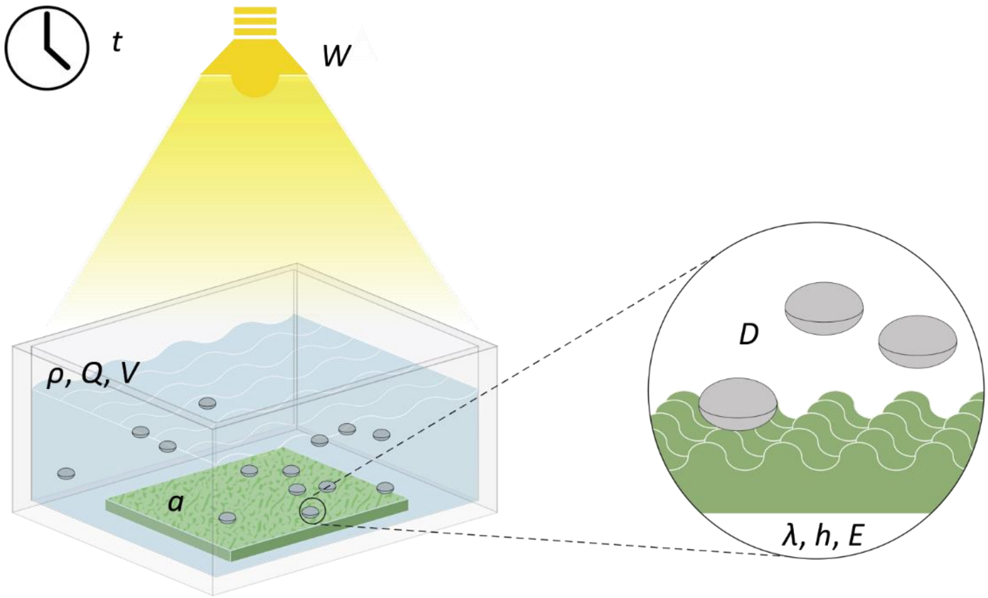
t
W
ρ, Q, V
a
D
λ, h, E

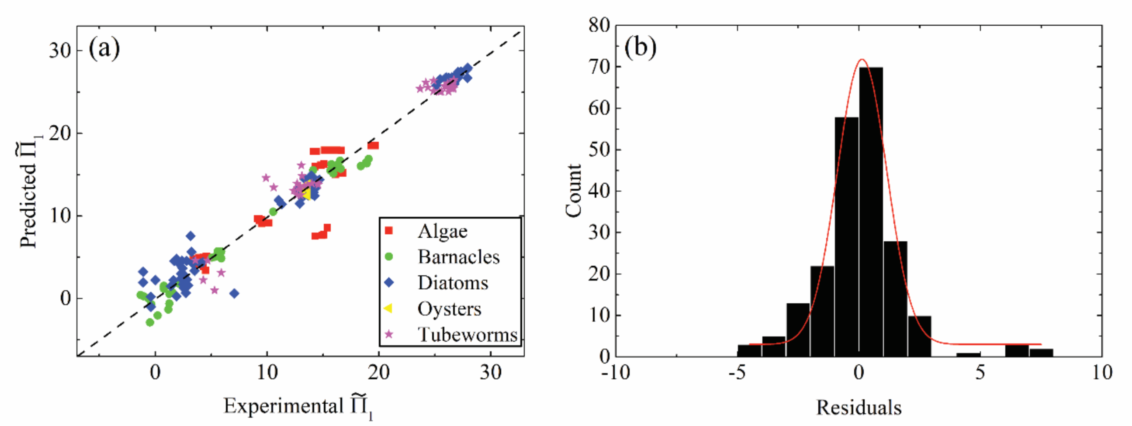
(a)
Predicted $\widetilde{\Pi}_1$
Experimental $\widetilde{\Pi}_1$
Algae
Barnacles
Diatoms
Oysters
Tubeworms
(b)
Count
Residuals

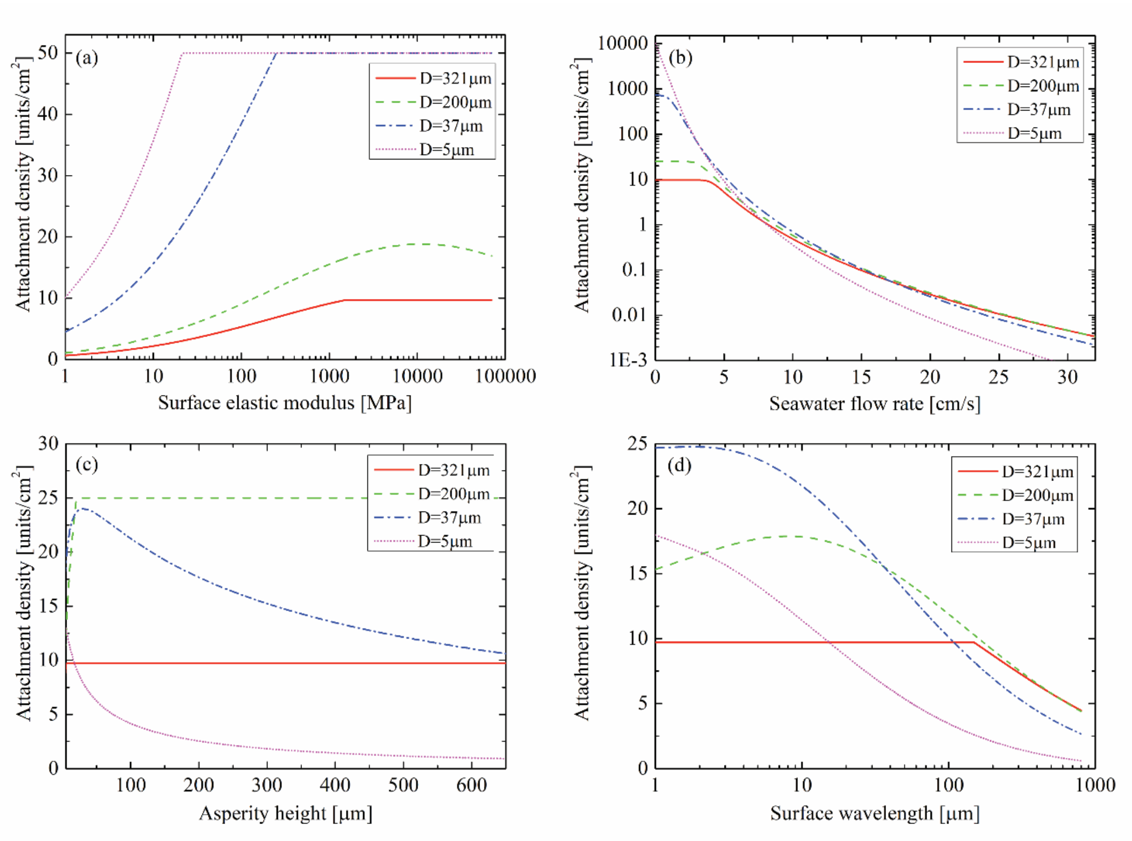
(a)
Attachment density [units/cm^2]
Surface elastic modulus [MPa]
D=321μm
D=200μm
D=37μm
D=5μm
(b)
Attachment density [units/cm^2]
Seawater flow rate [cm/s]
(c)
Attachment density [units/cm^2]
Asperity height [μm]
(d)
Attachment density [units/cm^2]
Surface wavelength [μm]

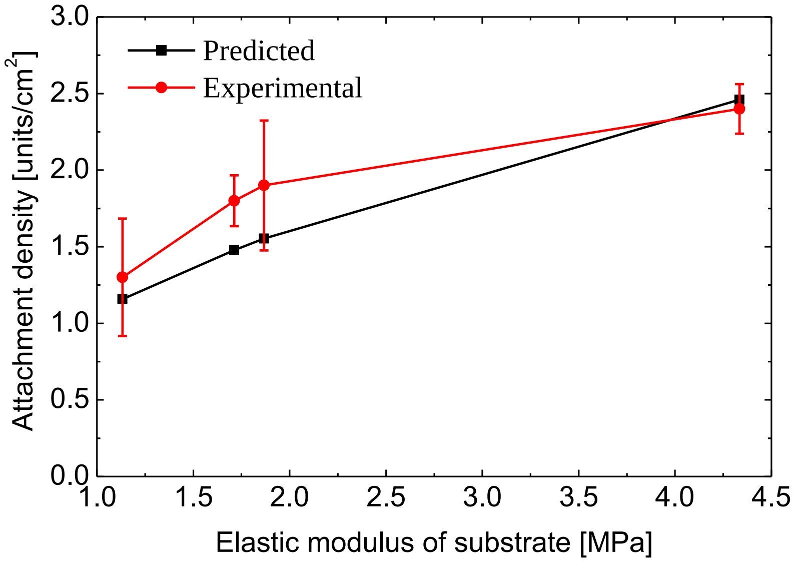

Predicted
Experimental
Attachment density [units/cm^2]
Elastic modulus of substrate [MPa]
0.0
0.5
1.0
1.5
2.0
2.5
3.0
1.0
1.5
2.0
2.5
3.0
3.5
4.0
4.5

Figure 1. Schematics showing the setup of a laboratory settlement experiment.

Figure 2. (a) Theoretically predicted $\widetilde{\Pi}_1$ versus experimental ones. The lack of apparent pattern for different organisms (algae, barnacles, diatoms, oysters, and tubeworms) implies the species independence of our model. (b) Histogram of the residuals of $e_m = \widetilde{\Pi}_{1,m} - \widetilde{\widetilde{\Pi}}_{1,m}$ and the corresponding fitting curve of Gaussian distribution (mean μ =0.12, standard deviation $\sigma = 1.02$).

Figure 3. Effects of different influencing factors on attachment density predicted by theoretical model: (a) surface stiffness, (b) seawater flow rate, (c) asperity height and (d) surface wavelength. Following parameters are taken constant in each case: (a) $h = \lambda = 0$, $W = 7.95$ Wm^{-2}, $Q = 0$, $V = 10$ ml, $\rho = 5$ ml^{-1}, $t = 48$ h; (b) $E = 2$ MPa, $h = \lambda = 10$ µm, $W = 7.95$ Wm^{-2}, $V = 1000$ ml, $\rho = 10$ ml^{-1}, $t = 48$ h; (c) $E = 2$ MPa, $\lambda = 10$ µm, $W = 7.95$ Wm^{-2}, $V = 10$ ml, $\rho = 10$ ml^{-1}, $t = 48$ h; (c) $E = 2$ MPa, $h = 10$ µm, $W = 7.95$ Wm^{-2}, $V = 10$ ml, $\rho = 10$ ml^{-1}, $t = 48$ h.

Figure 4. Effect of substrate stiffness on the attachment density of tubeworms.